Aeration and deaeration at bottom aeration devices on spillways

HUBERT CHANSON
Department of Civil Engineering, The University of Queensland, Brisbane QLD 4072, Australia

Received June 25, 1993
Revised manuscript accepted November 9, 1993

Aeration devices are introduced along chute spillways and at bottom outlets to prevent cavitation damage in high velocity flows. Bottom aerators are characterized by large quantities of air entrained along the jet interfaces and also by a strong deaeration process near the impact of the water jet with the spillway bottom. In this paper, the aeration and deaeration occurring respectively in the aeration region and in the impact region are reviewed. A reanalysis of air concentration data obtained on models provides information on the flow characteristics at the end of the impact region. These results enable an accurate initialization of the downstream flow calculations using the method developed by Chanson.

Key words: bottom aeration devices, aerators, spillways, air entrainment, detrainment.

Les aérateurs de fond sont utilisés sur les coursiers d'évacuateurs de crues de surface, et sur les vidanges de fond, pour éliminer les risques d'érosion par cavitation, pour des écoulements à grandes vitesses. Les aérateurs de fond sont caractérisés par un entraînement d'air très important le long des interfaces du jet et aussi par une désaération dans la zone d'impact du jet Cet article décrit les deux phénomènes. On y présente une nouvelle analyse de mesures expérimentales de concentrations en air, obtenues sur des modèles d'aérateurs. Ces résultats permettent une meilleure estimation des conditions d'écoulement à la fin de la zone d'impact, permettant ainsi de faire des calculs dans la zone d'écoulement aval, en utilisant la même méthode que Chanson.

Mots clés : aérateurs de fond, aérateurs, évacuateurs de crues, entraînement d'air, désaération.

Can. J. Civ. Eng. **21**, 404–409 (1994)

Introduction

On chute spillways and bottom outlets, cavitation damage may occur at clear water velocities of between 12 and 15 m/s. The damaging effects of cavitation erosion may be reduced or eliminated by (*i*) decreasing the critical cavitation number (e.g., removal of surface irregularities), (*ii*) increasing the cavitation resistance of the material surface (e.g., use of steel fibre concrete), (*iii*) using a combination of the first two methods (e.g., use of steel linings), (*iv*) directing the cavitation bubble collapses away from the solid boundaries, and (*v*) inducing flow aeration. With velocities greater than 20–30 m/s, the tolerances of surface finish required to avoid cavitation are too severe (Falvey 1990) and the cost of cavitation resistant materials is prohibitive. For these reasons, it becomes usual to protect the spillway surface from cavitation erosion by introducing air next to the spillway surface using aeration devices located at the spillway bottom and sometimes on the sidewalls (Fig. 1).

Experiments performed by Peterka (1953) and Russell and Sheehan (1974) in Venturi test sections showed that 5–10% of air was required to protect concrete specimens of 10–20 MPa compressive strength. On large chute spillways, field experiments performed by Deng (1988), Zhou and Wang (1988), and Zhang (1991) indicated that 4–8% of air concentration next to the spillway floor prevented erosion for velocities up to 44 m/s.

In this paper, the mechanisms of flow aeration above an aerator are described. Then the deaeration process occurring in the impact region is discussed and an analysis of air concentration data is presented. The results are later discussed and applied to downstream flow calculations.

NOTE: Written discussion of this paper is welcomed and will be received by the Editor until October 31, 1994 (address inside front cover).

Printed in Canada / Imprimé au Canada

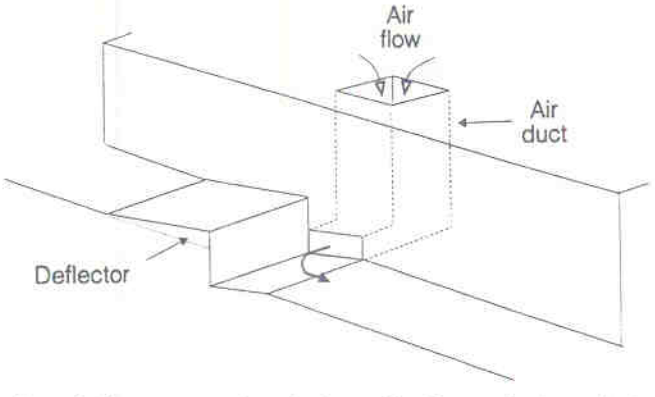

FIG. 1. Bottom aeration device with air supply through the sidewalls.

Air entrainment at a bottom aeration device

A small deflection in a chute structure (e.g., ramp, offset) tends to deflect the spillway flow away from the chute surface (Figs. 1 and 2). In the cavity formed below the nappe, a local subpressure (ΔP) is produced by which air is sucked into the flow (Q_{air}^{inlet}). The main flow regions above a bottom aerator are (*i*) the approach flow region which characterizes the initial nappe flow conditions, (*ii*) the transition region which coincides with the length of the deflector, (*iii*) the aeration region, (*iv*) the impact point region, and (*v*) the downstream flow region (Fig. 2) (Chanson 1989*a*; Kells and Smith 1991).

Flow aeration at an aerator

In the aeration region, air is entrained through both the upper and lower jet interfaces and by plunging jet entrainment at the intersection of the jet with the recirculating pool formed at the end of the cavity (Fig. 2). Chanson (1989*a*) showed the existence of an air recirculation process in the

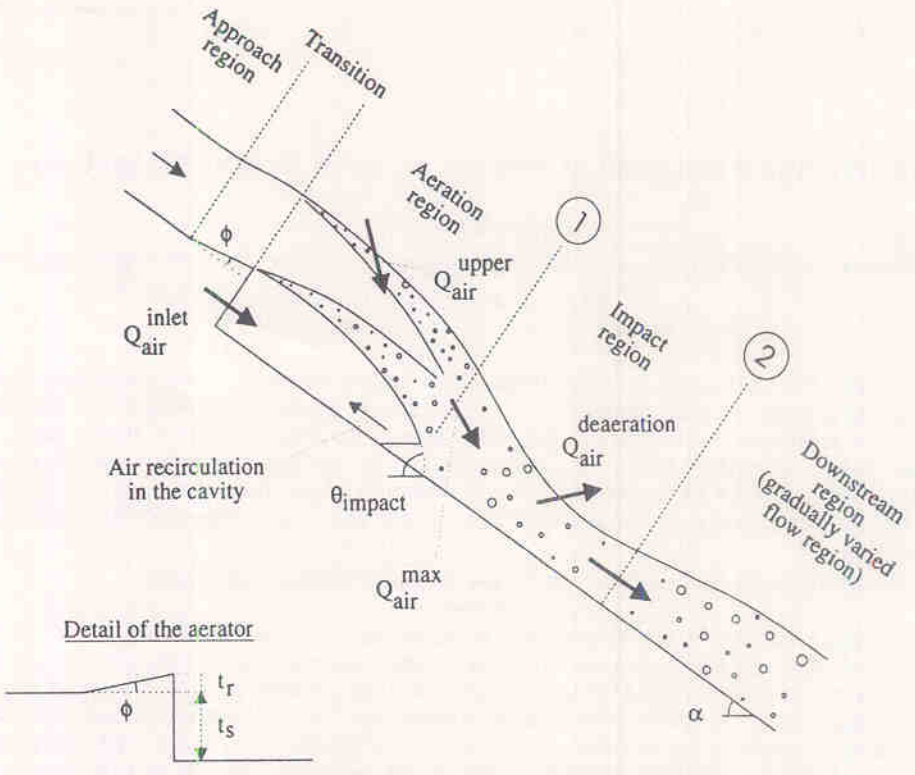

FIG. 2. Flow region above a bottom aeration device.

cavity below the jet. The continuity equation for air applied to the aeration region yields

$$[1] \quad Q_{air}^{max} = Q_{air}^{upper} + Q_{air}^{inlet} + (Q_{air})_o$$

where Q_{air}^{max} is the quantity of air entrained at the end of the jet (section 1, Fig. 2), Q_{air}^{upper} is the net air entrainment at the upper free surface of the jet, Q_{air}^{inlet} is the air discharge supplied by the air supply system, and $(Q_{air})_o$ is the initial free-surface aeration at the end of the deflector.

The air discharge supplied by the air inlets, Q_{air}^{inlet}, and the cavity subpressure, ΔP, are deduced from the duct head losses and the air entraining capacity of the flow above the aerator[1] (Low 1986; Rutschmann et al. 1986). These calculations fix the air discharge supplied by the inlets, the underpressure in the cavity beneath the jet and hence the jet trajectory.

Chanson (1991) analyzed the diffusion equation of air bubbles at the free surface and developed an analytical solution of the upper nappe entrainment as

$$[2] \quad \frac{Q_{air}^{upper}}{Q_w} = K_o \left[\frac{L}{d_o} \tan \psi^U - 2 \frac{(Q_{air})_o}{Q_w} \log_e \left(1 + \frac{1}{2} \frac{\tan \psi^U}{(Q_{air})_o / Q_w} \frac{L}{d_o} \right) \right] - 0.90 \frac{L}{d_o} \frac{u_r}{(U_w)_o} \cos \alpha$$

where $K_o = 0.1755$, Q_w is the water discharge, L is the distance from the end of the deflector, u_r is the rise velocity of air bubbles subject to a negative pressure gradient (Chanson 1989*a*, 1991), d_o and $(U_w)_o$ are the flow depth and velocity at the end of the deflector, and ψ^U is the lateral spread of the jet. Chanson (1991) indicates that for low pressure gradient, the angle of the jet spread may be estimated as $\psi^U = 0.75°$, but when the air inlets are sealed, the spread angle might be expected to be a function of the pressure gradient.

The knowledge of Q_{air}^{inlet} and Q_{air}^{upper} ([2]) enables the estimation of the flow aeration, Q_{air}^{max}, at the end of the jet ([1]).

Deaeration in the impact region

In the impact point region, the flow is subject to a rapid change of pressure distribution from a negative pressure gradient above the nappe to a maximum pressure gradient at the impact point (Fig. 3). The analysis of the experiments detailed in Table 1 shows consistently a strong de-strong deaeration process occurring in the impact region. Figure 4 shows a typical example of the quantity of air entrained within the flow as a function of the distance from the end of the deflector. The strong deaeration process is highlighted in the figure. Equation [2] is also plotted in Fig. 4 and compared with the data. It is worth noting that, in Fig. 4, further aeration takes place in the downstream flow region. Indeed, the author (Chanson 1989*b*) showed that the downstream flow behaves as a self-aerated flow: the air content will tend toward the uniform equilibrium mean concentration, i.e., $C_e = 0.65$ and $(Q_{air}/Q_w)_e = 1.86$ for $\alpha = 52.3°$, in Fig. 4.

The quantity of air escaping in this region is a function of the jet velocity at the impact, V_{impact}; the jet thickness at the impact, d_{impact}; the gravity; the angle of the water jet with the spillway floor at the impact ($\theta_{impact} - \alpha$); the channel slope, α; and the quantity of air entrained at the end of the jet, Q_{air}^{max}. Dimensional analysis yields the following:

$$[3] \quad \frac{Q_{air}^{deaeration}}{Q_{air}^{max}} = F\left(\frac{V_{impact}}{\sqrt{g d_{impact}}}; \theta_{impact} - \alpha; \alpha \right)$$

[1]The air entraining capacity of the flow above the aerator is called the air demand and is defined as the relationship between the air discharge supplied by the air inlets, the cavity subpressure, and the flow characteristics.

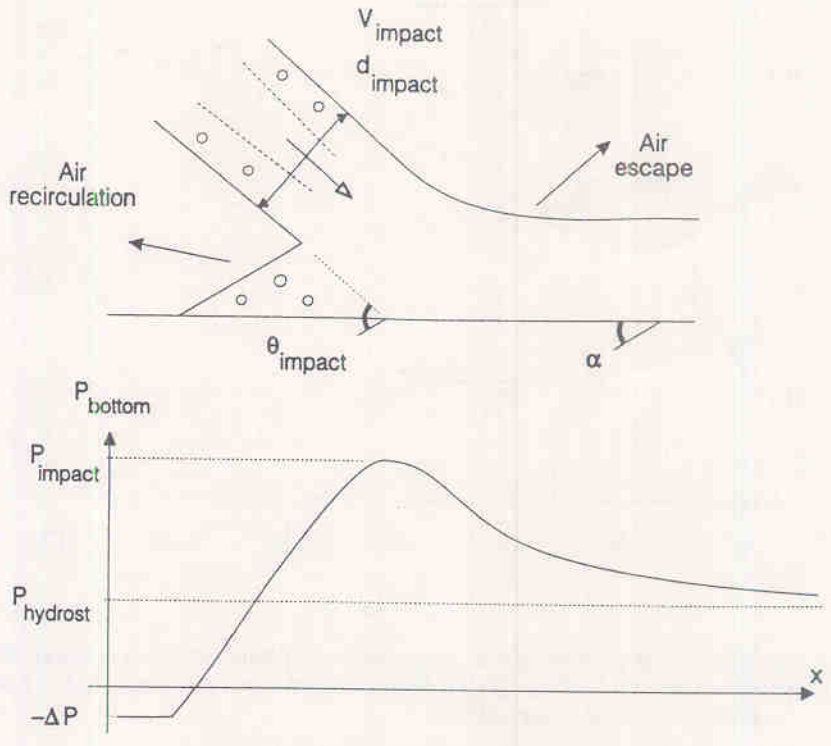

FIG. 3. Impact point region.

where $Q_{air}^{deaeration}$ is the detrainment in the impact region.

The angle of the jet with the spillway bottom can be deduced from jet trajectory calculations. Using the method of Tan (1984), it can be estimated as

$$[4a] \quad \tan(\theta_{impact} - \alpha) = \tan\phi \sqrt{1 + 2\frac{(t_r + t_s)g(\cos\alpha + P_N)}{(U_w)_o^2(\sin\phi)^2}}$$

(aerator with ramp)

$$[4b] \quad \tan(\theta_{impact} - \alpha) = \sqrt{2t_s\frac{g(\cos\alpha + P_N)}{(U_w)_o^2}}$$

(aerator without ramp)

where ϕ is the ramp angle, t_r is the ramp height, t_s is the offset height, and $P_N = \Delta P/(\rho_w g d_o)$.

The author reanalyzed the air concentration data obtained by Shi et al. (1983), Cui (1985), Low (1986), and Chanson (1988). Details of the experiments are reported in Table 1. For these data, the deaeration process is primarily a function of the angle of impact of the jet with the channel bottom $(\theta_{impact} - \alpha)$, and [3] becomes

$$[5] \quad \frac{Q_{air}^{deaeration}}{Q_{air}^{max}} = 0.0762(\theta_{impact} - \alpha)$$

where the angles θ_{impact} and α, defined in Fig. 2, are in degrees. Equation [5] is compared with the experimental data in Fig. 5 where the impact angle $(\theta_{impact} - \alpha)$ is computed using [4]. It must be noted that, for the experiments of Shi et al. (1983) and Cui (1985), the subpressure in the cavity beneath the nappe was deduced from the work of Pan et al. (1980) on the same spillway model.

The flow aeration at the end of the impact region (section 2, Fig. 2) is then $Q_{air}^{max} - Q_{air}^{deaeration}$ and can be computed using [1] and [5]. The mean air concentration[2] at the end of the impact region, C^*, is given by

$$[6] \quad C^* = \frac{Q_{air}^{max} - Q_{air}^{deaeration}}{Q_w + Q_{air}^{max} - Q_{air}^{deaeration}}$$

In the impact region, high momentum losses occur (Chanson 1989*a*). The data of Shi et al. (1983), Cui (1985), Low (1986), and Chanson (1988) suggest that the flow depth, d^*, at the end of the impact region (i.e., section 2, Fig. 2) may be estimated as

$$[7] \quad \frac{d^*}{d_{impact}} = 1.92 - 0.135(\theta_{impact} - \alpha)$$

where θ_{impact} and α are in degrees, and d_{impact} is the jet thickness at the end of the jet (i.e., section 1, Fig. 2; see also Fig. 3). Equation[7] is compared with the experimental data in Fig. 6.

Discussion

Figures 4 and 5 show that up to 80% of the flow aeration taking place along the jet can be lost in the impact region. Figure 5 and equation [6] emphasize the correlation between the detrainment and the impact angle of the jet with the channel bed. As a consequence, designers should consider aerator geometries that minimize the impact angle, for example, aerator with offset only or flat ramp, modification of the channel slope in the vicinity of the jet impact.

Further, an appropriate choice of the aerator operating conditions can reduce the impact angle and hence the detrainment. For a given aerator geometry, jet trajectories for low cavity subpressures provide shallower impact angles. But

[2]The mean air concentration and the quantity of air entrained within the flow are related by $Q_{air}/Q_w = C_{mean}/(1 - C_{mean})$.

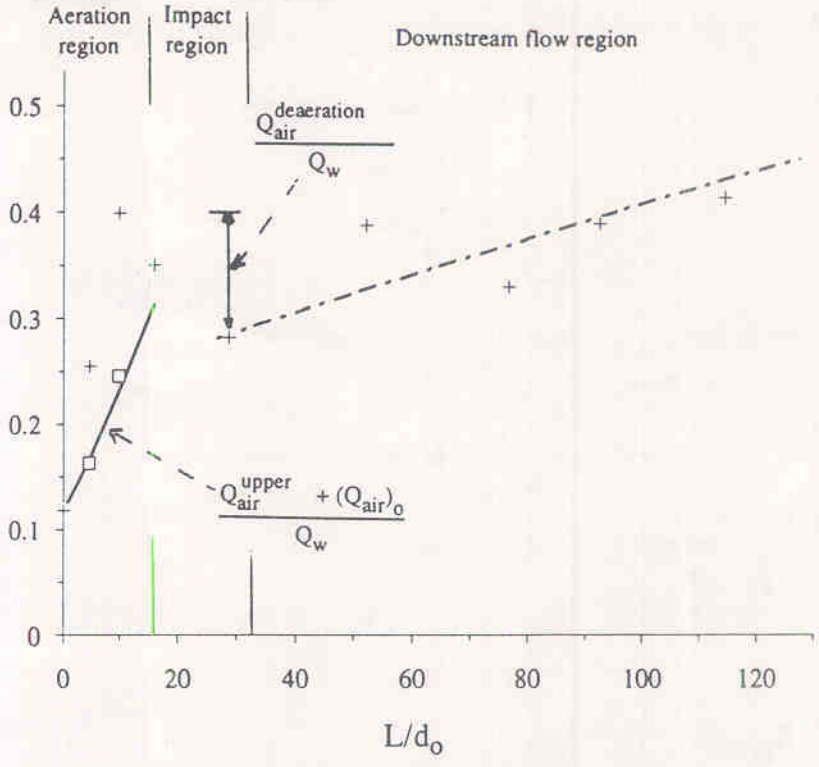

FIG. 4. Quantity of air entrained above an aeration device: comparison of experimental data (Chanson 1988, Run 873-2), equation [2] and downstream flow calculations as Chanson (1989*b*). Q_w = 0.0683 m^3/s and d_o = 0.0313 m. +, Q_{air}/Q_w data; □, $[(Q_{air})_{upper}+(Q_{air})_o]/Q_w$ data; ——, eq. [2]; and – – –, downstream flow computations.

TABLE 1. Aerator configurations for air concentration measurements

Reference (1)	Slope (°) (2)	Offset height t_s (m) (3)	Ramp height t_r (m) (4)	Ramp angle (°) (5)	No. of experiments (6)	W (m) (7)	d_o (m) (8)	Fr_o (9)	P_N (10)
Shi et al. (1983)	49.0	0.0	0.015	5.7	1	0.20	0.058	18.6	1.0*
Cui (1985)	0.0	0.0	0.015	5.7	1	0.20	0.120	8.9	0.8*
	30.0				1		0.150	6.0	1.0*
	49.0				1		0.120	7.5	1.1*
Low (1986)	51.30	0.030	0.030	5.7	5	0.25	0.050	6–13.5	0–0.06
Chanson (1988)	52.33	0.030	0.0	0.0	2	0.25	0.023	19.5	0.01–0.5
					12		0.035	10.5–19.5	0–1.6
					2		0.081	6.0	0.07–0.3

*Estimated from the experiments of Pan et al. (1980).

the achievement of low cavity subpressures requires smoother and larger air vents, which are generally more expensive.

Downstream flow region

In the downstream flow region, experimental data obtained on spillway models show consistently that air bubbles are redistributed downstream of an aeration device as in self-aerated flows (Shi et al. 1983; Cui 1985; Low 1986; Chanson 1988). Indeed, the flow is gradually varied and there is a complete analogy between the flow downstream of an aerator and self-aerated flows (Chanson 1989*b*; Falvey 1990; Hager 1992).

If the flow conditions at the end of the impact region (i.e., section 2, Fig. 2) are known ([6] and [7]), the flow characteristics at any point along the spillway can be computed using the same method as that developed by Wood (1985). Assuming a slow variation of the rate of air entrainment, a slow variation of the velocity with distance, and a quasi-hydrostatic pressure gradient, the continuity equation for air and the energy equation provide two simultaneous equations in terms of the mean air concentration and the flow depth (Chanson 1989*b*, 1993). For the data of Shi et al. (1983), Cui (1985), Low (1986), and Chanson (1988), the start of the downstream region (i.e., section 2 in Fig. 2) is located approximately at $1.5L_{jet}$ from the end of the deflector, where L_{jet} is the jet length.

Figure 7 shows an example of downstream flow calculations, where the mean air concentration, C_{mean}, and the flow depth, d, are plotted as a function of the dimensionless distance L/d_o from the end of the deflector. In Fig. 7, the computations were initialized using [4*b*], [6], and [7]. Other examples of applications were reported by Chanson (1988, 1989*b*).

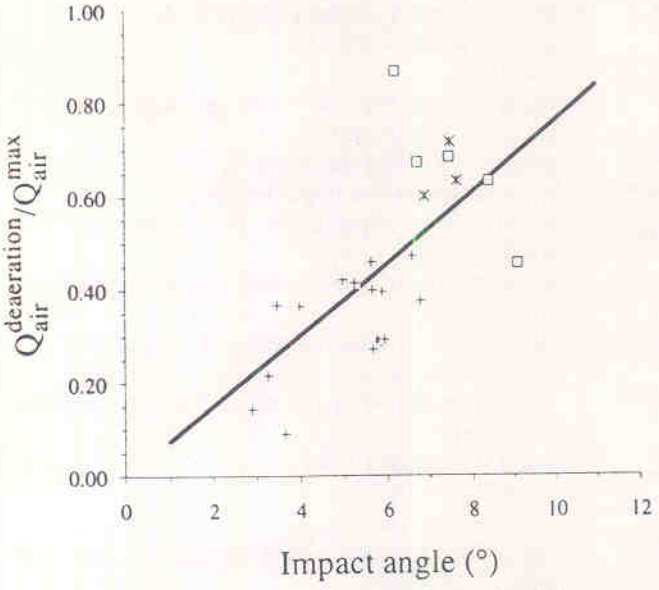

FIG. 5. Detrainment in the impact region ($Q_{air}^{degradation}/Q_{air}^{max}$) as a function of the impact angle ($\theta_{impact} - \alpha$) (Shi et al. 1983; Cui 1985; Low 1986; Chanson 1988). ●, Shi 1983; *, Cui 1985; □, Low 1986; +, Chanson 1988; and ——, eq. [6].

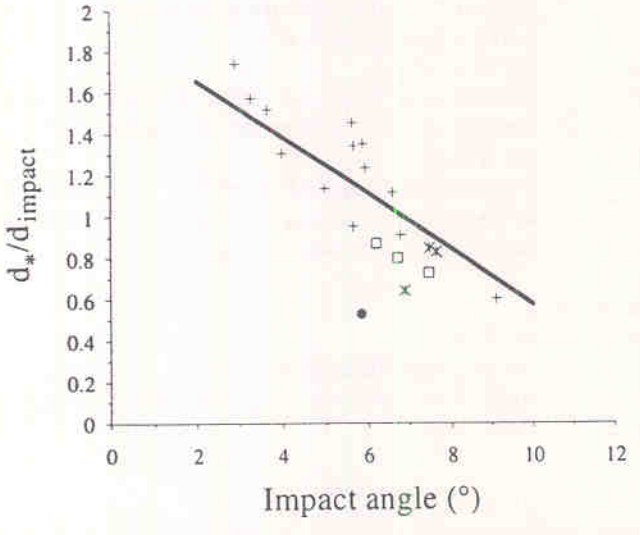

FIG. 6. Flow depth at the end of the impact point region as a function of the impact angle ($\theta_{impact} - \alpha$) (Shi et al. 1983; Cui 1985; Low 1986; Chanson 1988). ●, Shi 1983; *, Cui 1985; □, Low 1986; +, Chanson 1988; and ——, eq. [7].

Conclusion

Aeration devices are designed to introduce artificially air above spillways. In the aeration region, large quantities of air are entrained along the air–water interfaces of the jet. But a strong deaeration occurs near the impact of the nappe with the spillway bottom.

The flow aeration along the jet can be deduced from the aerator air demand and the upper free surface aeration, using the continuity equation for air ([1]). A reanalysis of air concentration data obtained on models (Table 1) indicate that a large detrainment process and high momentum losses occur in the impact region. To a first approximation, the flow conditions at the end of the impact region (Fig. 2, section 2) are primarily of function of the impact angle of the jet with the spillway bottom ([6] and [7]). The results provide the flow characteristics at the end of the impact region and enable flow calculations in the downstream flow region using an analogy with self-aerated flow calculations. Further, these results may be used to optimize the design of aerators with a reduction of the impact detrainment.

It must be emphasized that, in despite of the strong deaeration occurring in the impact point region, bottom aerators are very efficient devices for introducing large quantities of air over a short distance.

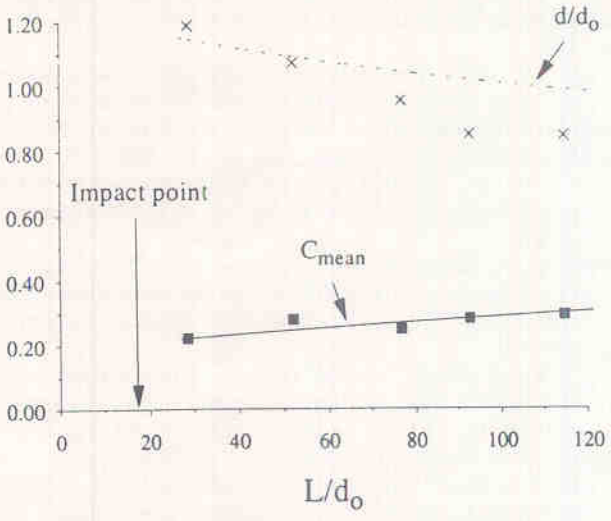

FIG. 7. Downstream flow region: comparison between calculations as Chanson (1989*b*, 1993) and data (Chanson 1988, Run 873-2). $Q_w = 0.0683$ m^3/s and $d_o = 0.0313$ m. - - -, d/d_o computed; ×, d/d_o data; ——, C_{mean} computed; and ■, C_{mean} data.

Chanson, H. 1988. A study of air entrainment and aeration devices on a spillway model. Ph.D. thesis, Department of Civil Engineering, University of Canterbury, Christchurch, New Zealand.

Chanson, H. 1989*a*. Study of air entrainment and aeration devices. Journal of Hydraulic Research, **27**(3): 301–319.

Chanson, H. 1989*b*. Flow downstream of an aerator. Aerator spacing. Journal of Hydraulic Research, **27**(4): 519–536.

Chanson, H. 1990. Study of air demand on spillway aerator. Journal of Fluids Engineering, **112**: 343–350.

Chanson, H. 1991. Aeration of a free jet above a spillway. Journal of Hydraulic Research, **29**(5): 655–667; **29**(6): 864.

Chanson, H. 1993. Self-aerated flows on chutes and spillways. ASCE Journal of Hydraulic Engineering, **119**(2): 220–243.

Cui, L. 1985. Air concentration distribution downstream of aeration ramp. Shuili Xuebao (Journal of Hydraulic Engineering), Beijing, China, **1**: 45–50 (in Chinese).

Deng, Z. 1988. Problems of flood relief/energy dissipation and high-velocity flow at Wujiangdu Hydropower Station. Proceedings of the International Symposium on Hydraulics for High Dams, International Association for Hydraulic Research, Beijing, China, pp. 230–238.

Falvey, H.T. 1990. Cavitation in chutes and spillways. United States Bureau of Reclamation Engineering Monograph, No. 42, Denver, Colo.

Hager, W.H. 1992. Spillways, shockwaves and air entrainment — review and recommendations. International Congress on Large Dams Bulletin, No. 81, January.

Kells, J.A., and Smith, C.D. 1991. Reduction of cavitation on spillways by induced air entrainment. Canadian Journal of Civil Engineering, **18**: 358–377; **19**: 924–929.

Low, H.S. 1986. Model studies of Clyde dam spillway aerators. Research Report No. 86-6, Department of Civil Engineering, University of Canterbury, Christchurch, New Zealand.

Pan, S.B., Shao, Y.Y., Shi, Q.S., and Dong, X.L. 1980. Self-aeration capacity of a water jet over an aeration ramp. Shuili Xuebao (Journal of Hydraulic Engineering), Beijing, China, No. 5, pp. 13–22 (in Chinese). (United States Bureau of Reclamation Translation No. 1868, Book No. 12,455, Paper No. 2.)

Peterka, A.J. 1953. The effect of entrained air on cavitation pitting. Joint Meeting Paper, International Association for Hydraulic Research and American Association of Civil Engineers, Minneapolis, Minn., August, pp. 507–518.

Russell, S.O., and Sheehan, G.J. 1974. Effect of entrained air on cavitation damaged. Canadian Journal of Civil Engineering, **1**: 97–107.

Rutschmann, P., Volkart, P., and Wood, I.R. 1986. Air entrainment at spillway aerators. Proceedings of the 9th Australasian Fluid Mechanics Conference, Auckland, New Zealand, December, pp. 350–353.

Shi, Q., Pan, S., Shao, Y., and Yuan, X. 1983. Experimental investigation of flow aeration to prevent cavitation erosion by a deflector. Shuili Xuebao (Journal of Hydraulic Engineering), Beijing, China, **3**: 1–13 (in Chinese).

Tan, T.P. 1984. Model studies of aerators on spillways. Research Report No. 84-6, University of Canterbury, Christchurch, New Zealand.

Wood, I.R. 1985. Air water flows. Proceedings of the 21st International Association for Hydraulic Research Congress, Melbourne, Australia, Keynote address, pp. 18–29.

Zhang, S. 1991. Latest developments in hydraulic design of outlet works in China. Bulletin Institutionen for Vattenbyggnad, Kungl Tekniska Hogskolan (Hydraulic Engineering, Royal Institute of Technology), Stockholm, Sweden, No. TRITA-VBI-154.

Zhou, L., and Wang, J. 1988. Erosion damage at Fengman spillway dam and investigation on measures of preventing cavitation. Proceedings of the International Symposium on Hydraulics for High Dams, International Association for Hydraulic Research, Beijing, China, pp. 703–709.

List of symbols

A	cross-sectional area (m^2)
C	air concentration defined as the volume of air per unit volume
C_{mean}	depth averaged air concentration defined as $(1 - Y_{90})C_{mean} = d$
C^*	mean air concentration at the end of the impact point region
d	characteristic depth (m) defined as $d = \int_0^{Y_{90}} (1 - C)\, dy$
d_{impact}	water jet thickness (m) at the impact
d_o	initial flow depth (m)
d^*	characteristic depth (m) at the end of the impact point region
Fr_o	Froude number defined as $Fr_o = (U_w)_o/\sqrt{gd_o}$
g	gravity constant (m/s^2)
K_o	constant
L	distance from the end of the deflector (m)
L_{jet}	water jet length (m)
P_N	pressure gradient number: $P_N = \Delta P/(\rho_w g d_o)$
$Q_{air}^{deaeration}$	detrainment in the impact region (m^3/s)
Q_{air}^{inlet}	air discharge supplied by the air inlet system (m^3/s)
Q_{air}^{max}	quantity of air entrained at the end of the jet (m^3/s)
$(Q_{air})_o$	initial free-surface aeration at the end of the deflector (m^3/s)
Q_{air}^{upper}	net air entrainment at the upper free surface of the jet (m^3/s)
Q_w	water discharge (m^3/s)
t_r	ramp height (m)
t_s	offset height (m)
$(U_w)_o$	mean flow velocity at the end of the approach flow region (m/s)
u_r	rise velocity of air bubbles (m/s)
V_{impact}	jet velocity at the impact (m/s)
W	channel width (m)
Y_{90}	characteristic depth (m) where the air concentration is 90%
y	distance from the bottom measured perpendicular to the spillway surface (m)
α	spillway slope
ΔP	difference between the pressure above the flow and the air pressure beneath the nappe (Pa)
ϕ	ramp angle
θ_{impact}	angle between the water jet and the horizontal at the impact of the jet with the spillway bottom
ψ^U	lateral spread of the upper jet free-surface

Subscript

air	air flow
e	uniform equilibrium flow region
o	initial flow condition in the approach flow region
w	water flow